



Laboratory investigation of mechanical behavior of granite samples containing discontinuous joints through direct shear tests

Xu-Xu Yang¹ · Pinnaduwa H. S. W. Kulatilake²

Received: 29 September 2018 / Accepted: 17 January 2019 / Published online: 24 January 2019
© Saudi Society for Geosciences 2019

Abstract

The effect of the normal stress and joint persistency on the mechanical behavior of granite samples containing discontinuous joints was investigated in the laboratory through direct shear tests. The test results revealed three different failure modes occurring at the rock bridge: (a) shear failure, (b) compressive-shear failure, and (c) tensile failure. The failure mode depends on the joint persistency and normal stress level and influences the peak shear strength. Moreover, the joint persistency and normal stress level were also found to have a considerable influence on the post-failure behavior such as the fracture roughness and residual shear strength based on rock bridge area. The conducted investigation provided better understanding of the effect of a rock bridge on mechanical behavior of granitic discontinuous joints towards estimating the resistance capacity of rock bridges and hence to allow evaluation of stability of rock masses in both surface and underground excavations in rock engineering.

Keywords Granite samples · Discontinuous joints · Rock bridge · Direct shear test · Mechanical properties

Introduction

Translational rock slides and instability of rock masses in engineering field may be associated with the shear failure of discontinuous rock joints (Zhao et al. 2015; Yang et al. 2016). This type of failure is a combination of sliding along joint sections and rupturing through intervening rock bridges. Discontinuous joints herein refer to rock discontinuities that are not fully developed as fully persistent joints with respect to the geological time. Discontinuous joints are commonly encountered in rock engineering. For instance, Lajtai et al. (1994) reported that they characterized two typical fracture patterns in the yield pillars of the potash mines of Saskatchewan, which are the en echelon tensile crack array and the en echelon shear crack array. These two types of cracks were the evidence of the existence of discontinuous

joints in engineering field problem. With increasing stress, the shear crack array often collapsed, forming the envelope or hourglass structures of the potash mine. Li et al. (2012) conducted in situ borehole camera monitoring of the failure evolution of surrounding rock masses having intermittent discontinuous joints with rock bridges in-between them in deeply buried tunnels of the Jinping II hydropower station. With the converging deformation of the surrounding rock masses, the discontinuous joints connected with each other by rupturing through the rock bridges and eventually failed by forming a macro-fracture. Above all, in rock masses, the joints are not always continuous and smooth, but sometimes contain rock bridges between the joint surfaces (Wong et al. 2002; Yang et al. 2017, 2018; Sharma et al. 2018; Yang and Qiao 2018). The rock bridges are thought to produce a considerable strength reserve in discontinuous joints. Paronuzzi et al. (2016) reported a back-analysis of a rock wedge failure (volume = 25–30 m³) that involved a limestone scarp in the Rosandra Valley in Trieste Karst, NE Italy. According to the field survey performed on the detachment surface, a single rock bridge having a size of about 15 cm × 30 cm has been determined. They found that the equilibrium of the wedge was temporarily attained due to the strength contribution provided by the rock bridge. Thus, the strength of the rock bridge contained in discontinuous joints has a significant influence on stabilization of rock engineering structures. Moreover, the

✉ Xu-Xu Yang
yangxu_skdrm@hotmail.com

¹ Shandong Provincial Key Laboratory of Civil Engineering Disaster Prevention and Mitigation, Shandong University of Science and Technology, Qingdao 266590, China

² Rock Mass Modeling and Computational Rock Mechanics Laboratories, University of Arizona, Tucson, AZ 85721, USA

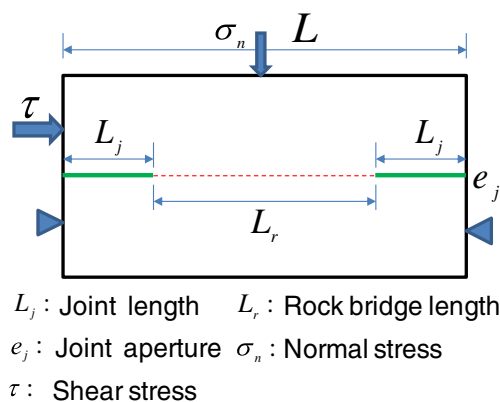


Fig. 1 The conceptual rock block model containing impersistent joints

rock bridges play an important role on the permeability of a rock mass due to the fact that even one tiny area of rock bridge can block the fluid-flow channel along a rock fracture. Therefore, the mechanical behaviors of discontinuous joints having rock bridges are supposed to deserve more research attention for optimizing rock stabilization designs associated with surface and underground rock mass structures.

The shear strength behavior of rock bridges that exists between discontinuous joints is considerably important in rock engineering, but not completely understood yet. Lajtai (1969) performed direct shear tests on rock blocks containing discontinuous joints and found three distinct failure mechanisms: failure in tension, failure in shear, and failure at ultimate strength. He also pointed out that the discontinuous joints constitute the potential slip surfaces, of which the stability is dependent on the shear resistance of rock bridges. Through physical experiments, Gehle and Kutter (2003) demonstrated that based on the direction of the initial cracks that occurred in rock bridges, the wing cracks grow either toward the distant tip of the adjacent initial cracks or directly toward the tip of the neighboring cracks. With respect to the former crack growing scenario, the rock bridges fracture to form rough joint surfaces with some asperities at the end of the test. Gerolymatou and Triantafyllidis (2016) demonstrated that the shear resistance of material containing discontinuous joints is not only dependent on the spacing but also on the orientation of the joints. Asadizadeh et al. (2018) carried out shear tests on discontinuous joints having both rock bridges and asperities. Accordingly, they claimed that the fracturing process of samples could be classified into three categories, namely, tensile cracking, shear cracking, and mixed mode tensile-shear cracking.

Even though some insightful knowledge has been obtained through the above-mentioned physical experiments, the artificial rock-like material may not replicate the mechanical behavior of natural rocks due to the difference in physical and mechanical properties. For instance, the ratios of the uniaxial compressive strength to tensile strength of artificial materials used by Asadizadeh et al. (2018) and Gerolymatou and Triantafyllidis (2016) are only 6.70 and 5.45, respectively; on the other hand, for intact rock materials, this ratio could be as high as 10–20. Moreover, the most studies have placed the emphasis on the failure stage, i.e., failure mode and peak shear strength. Investigations performed on the post-failure behavior are rare. For instance, once the rock bridge between the discontinuous joints fail, it would change the rock bridge to a rough joint having a certain asperity configuration. Such a created fracture has significant influence on the mechanical and hydraulic behavior of the joint plane (Barton 1973; Bahaaddini et al. 2013, 2017; Ban et al. 2018), and thus play an important role in engineering performance of underground structures and the stability of rock slopes (Wu et al. 2018). Therefore, direct shear tests of granite samples containing discontinuous joints with different joint persistency were carried out under various normal stress levels to investigate the mechanical behavior of granitic discontinuous joints at the failure and post-failure stages. The present study aims to provide further understanding towards estimating the resistance capacity of discontinuous joints having rock bridges and hence to allow evaluation of stability of rock masses in both surface and underground rock engineering.

Sample preparation and test program

A conceptual model for a rock block having impersistent joints is displayed in Fig. 1. To describe the geometrical property of this rock block structure, the joint persistency, k , which is used to state the percentage of joint continuity, is defined by the rock bridge length, L_r , and the joint length, L_j , as follows:

$$k = \frac{2L_j}{L_r + 2L_j} = \frac{2L_j}{L} \quad (1)$$

When $0 < k < 1$, the discontinuity plane includes two separate joints with a solid rock bridge. A granitic rock material

Table 1 Mechanical property values of the granitic rock used for tests

Property	Density (g/cm^3)	UCS (MPa)	Tensile strength (MPa)	Young's modulus (GPa)	Poisson's ratio	Friction angle (degrees)	Cohesion (MPa)
Value	2.61	87.80	6.82	21.48	0.16	33.5	23.4

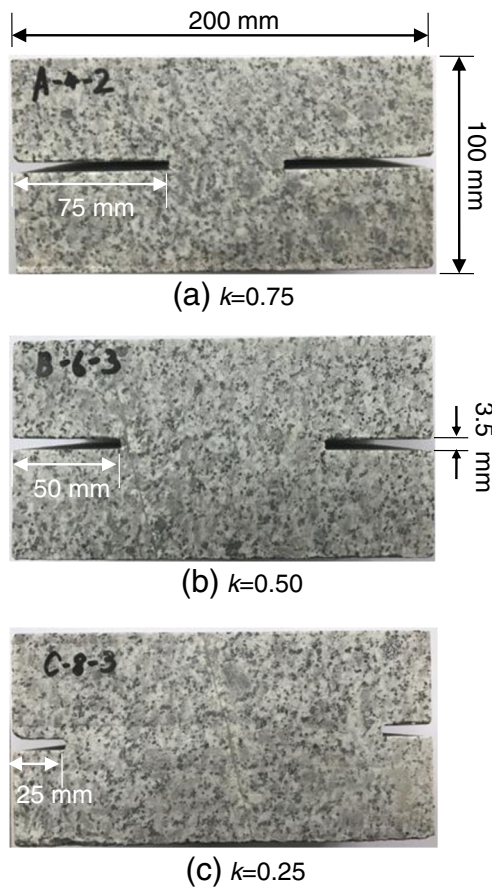


Fig. 2 Granite samples with impersistent joints having different joint persistency: **a** $k = 0.75$; **b** $k = 0.50$; **c** $k = 0.25$

collected from a quarry in Qingdao City, Shandong Province of China, was used to prepare the experiment samples according to the above-mentioned conceptual model. The selected granite is a coarse-grained medium hard rock with an average density of about 2.61 g/cm^3 . The main minerals are quartz, alkaline feldspar, plagioclase, and muscovite. Cylindrical samples with the diameter 50 mm and height 100 mm were carefully drilled and polished for estimating the mechanical properties of the granite according to the ISRM standards (ISRM 1978). The corresponding mechanical property values obtained for the granitic rock used for tests are listed in Table 1.

The granitic samples used for the direct shear tests were prismatic with dimensions of length 200 mm \times width

100 mm \times height 100 mm and internal structure as shown in Fig. 1. A high-pressure water jet cutting machine was utilized to create side notches (joints) at half height of each sample, as implied in Fig. 2. The joints were designed to be open with an aperture of 3.5 mm for simplification. The lengths of joint were 75 mm, 50 mm, and 25 mm, with correspondence to the joint persistency, k , being 0.75, 0.50, and 0.25, respectively. The granitic samples were then tested under normal stress levels being 2.0 MPa, 4.0 MPa, 6.0 MPa, and 8.0 MPa, respectively. In order to check the repeatability of test results, three same samples were experimented for each testing scenario, i.e., with the same joint persistency and under the same normal stress. Table 2 summarizes the sample information of the conducted direct shear tests.

A self-designed JAW-600 shear-flow coupled testing machine available at the Shandong University of Sciences and Technology (see Fig. 3a) was used to conduct these direct shear tests. By using the hydraulic actuators equipped with servo valves, the shear and normal loads were applied to the prepared samples. This machine was designed to bear a loading capacity of 600 kN in both shear and normal directions. In addition, the displacements along the shear and normal loading directions were recorded through LVDTs. The direct shear tests were implemented in displacement-controlled conditions by applying a constant loading rate of 0.15 mm/min to guarantee a quasi-static state during the test, which helps to capture the failure process. The termination criterion used for the testing was that the displacement should be continued until the sample fails and reach a steady residual state in the post-failure stage. The shear and normal loads and deformations were recorded simultaneously during the tests and the failure process of each sample was captured using a high-frequency video system (see Fig. 3b).

Shear stress-shear displacement behavior

Figures 4 and 5 show the shear stress-shear displacement curves obtained for jointed granitic samples. The shear stress-shear displacement curves of the granite samples having discontinuous joints with different joint persistency (k) subjected to different normal stress levels (σ_n) show significant differences. Figure 4a, b demonstrates that, for the same joint persistency, the peak shear stress of the shear stress-shear

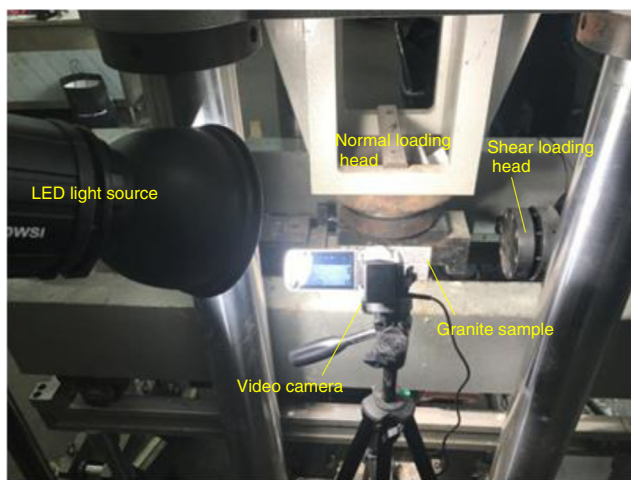
Table 2 Information of samples used for the direct shear tests

Test scenario	$\sigma_n = 2 \text{ MPa}$	$\sigma_n = 4 \text{ MPa}$	$\sigma_n = 6 \text{ MPa}$	$\sigma_n = 8 \text{ MPa}$
$k = 0.75$	A-2-1, A-2-2, A-2-3	A-4-1, A-4-2, A-4-3	A-6-1, A-6-2, A-6-3	A-8-1, A-8-2 , A-8-3
$k = 0.50$	B-2-1, B-2-2, B-2-3	B-4-1, B-4-2 , B-4-3	B-6-1 , B-6-2, B-6-3	B-8-1, B-8-2, B-8-3
$k = 0.25$	C-2-1, C-2-2 , C-2-3	C-4-1 , C-4-2, C-4-3	C-6-1, C-6-2, C-6-3	C-8-1 , C-8-2, C-8-3

A, B, and C stand for the joint persistency of 0.75, 0.50, and 0.25, respectively; the middle number provides the applied normal stress value, while the last number implies the number of replicates under the same test scenario. The number of the sample providing the representative result for each scenario is highlighted in bold format



(a) JAW-600 shear machine

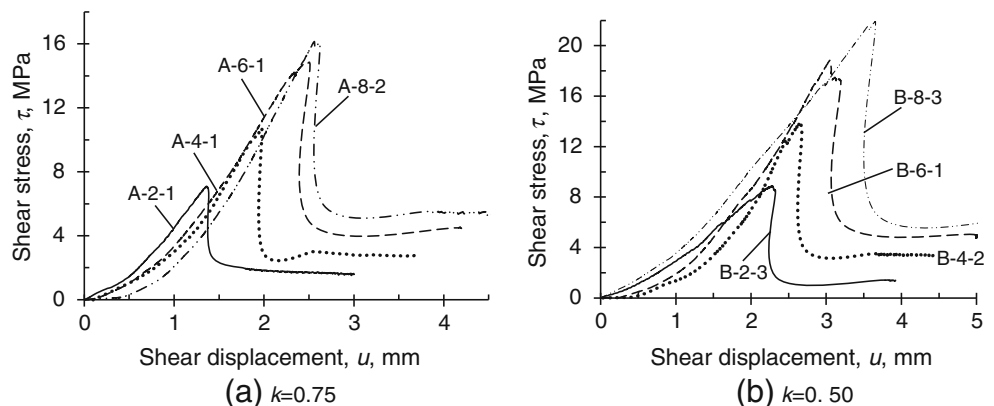


(b) high-frequency video system

Fig. 3 Testing apparatus and monitoring system used for direct shear testing

displacement curves increases gradually with increasing normal stress level. On the other hand, Fig. 5a, b indicates that by changing the joint persistency of rock block models, the shear stress-shear displacement behavior varies remarkably even under the same normal stress level.

Fig. 4 Effect of normal stress on the shear stress-shear displacement curves of granite samples containing discontinuous joints: **a** $k = 0.75$; **b** $k = 0.50$

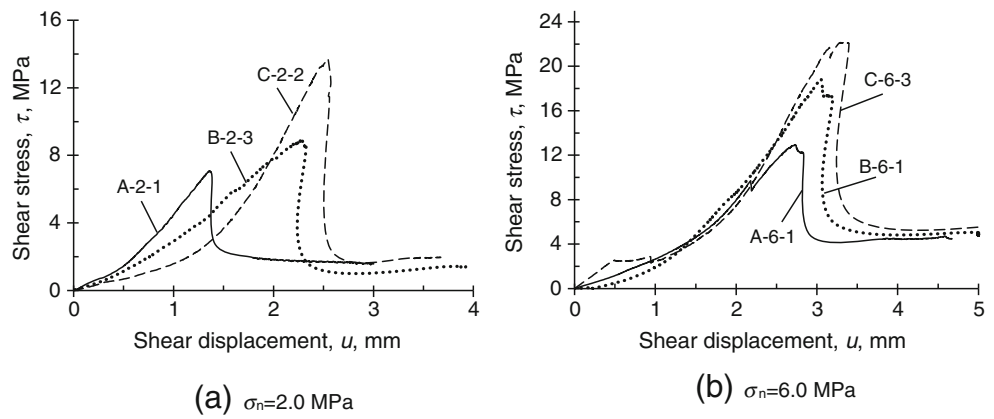


Laboratory experimental results usually display discrepancy for any two samples having the same scale even under the same testing conditions due to the heterogeneity of the rock material. Figure 6 shows the influence of heterogeneity on the shear stress-shear displacement curves of the rock samples having discontinuous joints under the same joint persistency and same normal stress level. The figure shows that the influence of the heterogeneity on the shear behavior depends on the joint persistency level. In other words, the influence of the heterogeneity on the shear behavior depends on the rock bridge length. When the joint persistency is high (e.g., $k = 0.75$), the shear stress-shear displacement curves for different samples show very good consistency (see Fig. 6a). When the joint persistency is low (e.g., $k = 0.25$), the shear stress-shear displacement curves for different samples show some discrepancy (see Fig. 6b). However, even for the samples with the lowest joint persistency of $k = 0.25$ (samples C-4-1, C-4-2, and C-4-3), the peak shear stress values are 15.87 MPa, 16.33 MPa, and 14.40 MPa, with deviations of 2.17%, 5.15%, and 7.28%, respectively, compared against the average peak shear stress value. That indicates that the heterogeneity has a negligible effect on the shear behavior of the tested granite samples containing discontinuous joints. In addition, the trends of the curves before and after peak stress for different samples also show good consistency.

Failure mode and peak shear strength

It is always of interest to look at the failure mode of the samples due to its dominant effect on the peak and post peak behavior of rock materials. Figure 7 shows the failure modes of the granite samples subjected to the direct shear tests. According to this figure, three different failure modes, (a) shear failure mode, (b) compressive-shear failure mode, and (c) tensile failure mode, were observed to occur at the rock bridges.

Fig. 5 Effect of joint persistency on the shear stress-shear displacement curves of granite samples containing discontinuous joints: **a** $\sigma_n = 2.0$ MPa; **b** $\sigma_n = 6.0$ MPa



- Shear failure mode: This failure mode occurs through the initiation of a crack from the tip of one pre-existing joint. The crack propagates directly to the tip of another joint and forms a planar failure surface. The failure surface is caused by a shear mechanism because crushed and pulverized materials were observed (Ghazvinian et al. 2012). This failure mode occurred for granite samples having large and medium joint persistency (e.g., $k = 0.75$ and 0.50) subjected to a relatively low normal stress (e.g., $\sigma_n = 2.0$ MPa and 4.0 MPa).
- Compressive-shear failure mode: Under relatively high normal stress, e.g., $\sigma_n = 6.0$ MPa and 8.0 MPa, the samples having large or medium joint persistency ($k = 0.75$ and 0.50) do not fail in a pure shear mechanism at the rock bridge between the discontinuous joints. As the shear load increases, the intact material adjacent to joint walls begins to fail to form a failure zone. This failure zone then extends through the rock bridge, which causes the rock bridge fragmented. It further propagates obliquely to the walls of another joint. The failure phenomenon is like that observed in a rock sample under compression. Moreover, after completion of the compression failure zone, a shear failure surface finally forms along the shear plane by leaving some crushed and pulverized materials. Therefore, this failure mode is named as the compressive-shear failure mode.

- Tensile failure mode: With reduction of joint persistency, taking $k = 0.25$ as an example, a splitting failure happens at the tip or wall of pre-existing discontinuous joints. The failure surface forms a curvilinear path through the rock bridge (Ghazvinian et al. 2012; Sarfarazi et al. 2014). It is caused by a tensile mechanism because no crushed or pulverized material was observed. Also, it is important to note that this failure mode does not depend on the normal stress.

According to Fig. 7, the joint persistency and normal stress level significantly influence the failure mode of granite samples and further influence the shear resistance capacity. Figure 8 and Table 3 depict the variation of the peak shear strength with the joint persistency and normal stress. Please note that although the pre-existing joints are open with a 3.5 mm initial aperture and may not contribute to shear resistance on the effective shear plane of the rock block model especially for the low normal stresses, the entire area along the shear plane including the joint area and rock bridge area was considered in computing the corresponding peak shear strength values (Cui 2012; Yang et al. 2016). At $\sigma_n = 2.0$ MPa, the peak shear strengths of the joint granite samples with joint persistency of 0.75 , 0.50 , and 0.25 are 7.09 MPa, 9.14 MPa, and

Fig. 6 Influence of heterogeneity on shear stress-shear displacement curves of the granite samples having the same joint persistency subjected to the same normal stress level: **a** $k = 0.75$, $\sigma_n = 4.0$ MPa; **b** $k = 0.25$, $\sigma_n = 4.0$ MPa

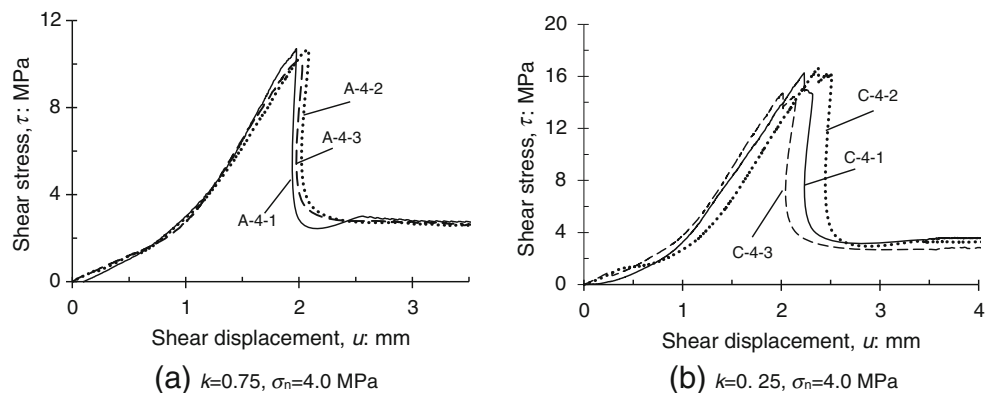
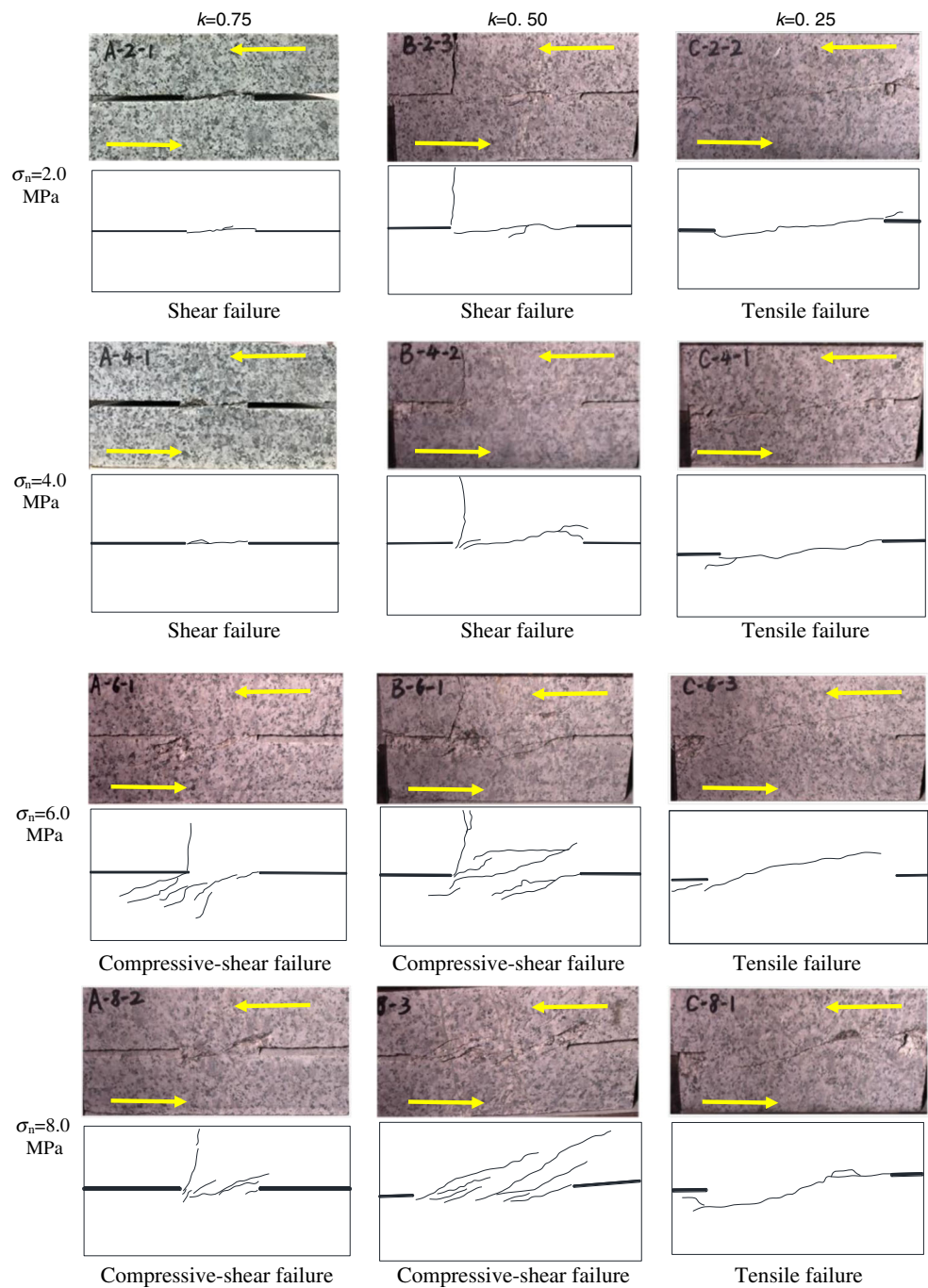


Fig. 7 Failure modes of granite samples with different joint persistency under different normal stress levels



13.52 MPa, respectively. When $\sigma_n=8.0$ MPa, the peak shear strengths of the joint granite samples are 16.13 MPa, 22.30 MPa, and 27.46 MPa, respectively. Therefore, the increment ratio of shear strength to normal stress, f_n ($f_n = \Delta\tau_p / \Delta\sigma_n$), is 1.51, 2.19, and 2.32 for joint persistency of 0.75, 0.50, and 0.25, respectively. According to the Mohr-Coulomb criterion, for intact rock material, the increment ratio of shear strength to normal stress would be $\tan\varphi_r$. According to Table 1, the f_n value

for the tested granitic rock would be 0.66, much less than the experimental values. These findings show that the normal stress enhances the shearing capacity of rock joints having rock bridges. This enhancement increases as the joint persistency decreases. This phenomenon might be due to the rock structure type of discontinuous joints with different persistency, and further demonstrates the significant effect of discontinuous joints on the mechanical behavior of granitic samples.

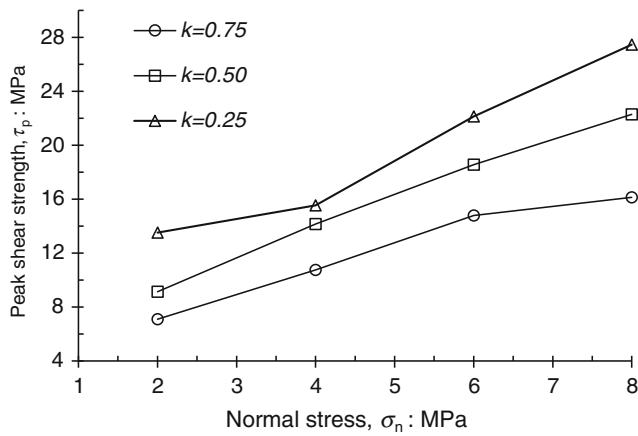


Fig. 8 Influence of the normal stress level and joint persistency on peak shear strength

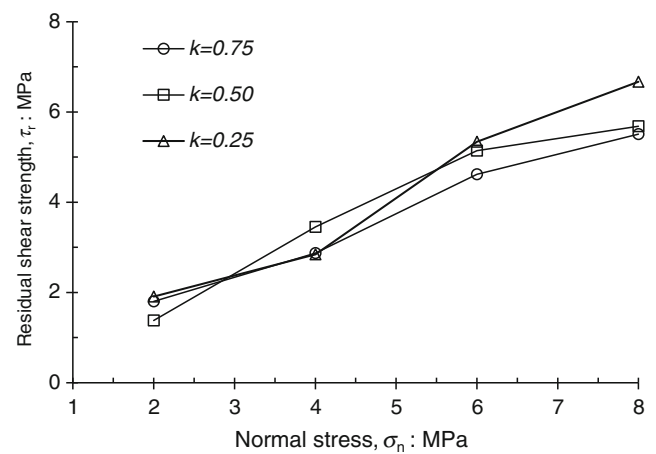


Fig. 9 Influence of the normal stress level and joint persistency on residual shear strength by considering the whole area of the rock joint

Residual shear strength and fracture roughness

In rock engineering, the rock bridges between the discontinuous joints may be considered as temporary rock structures because those fail under certain stress conditions (Shang et al. 2016). Once they fail, the shearing capacity of the joint may change significantly. Thus, it is of importance to look at the mechanical behavior of granite samples at the post-failure stage. Figure 9 and Table 3 depict the variation of the residual shear strength (based on the total area of the joint plane) with the joint persistency and normal stress. It can be seen from this figure that the residual shear strength generally increases with the normal stress increment. However, the joint persistency seems to have only a slight or negligible effect on the residual shear strength considering the same normal stress level. For example, at $\sigma_n = 2.0$ MPa, the residual shear strength values show very little difference even though

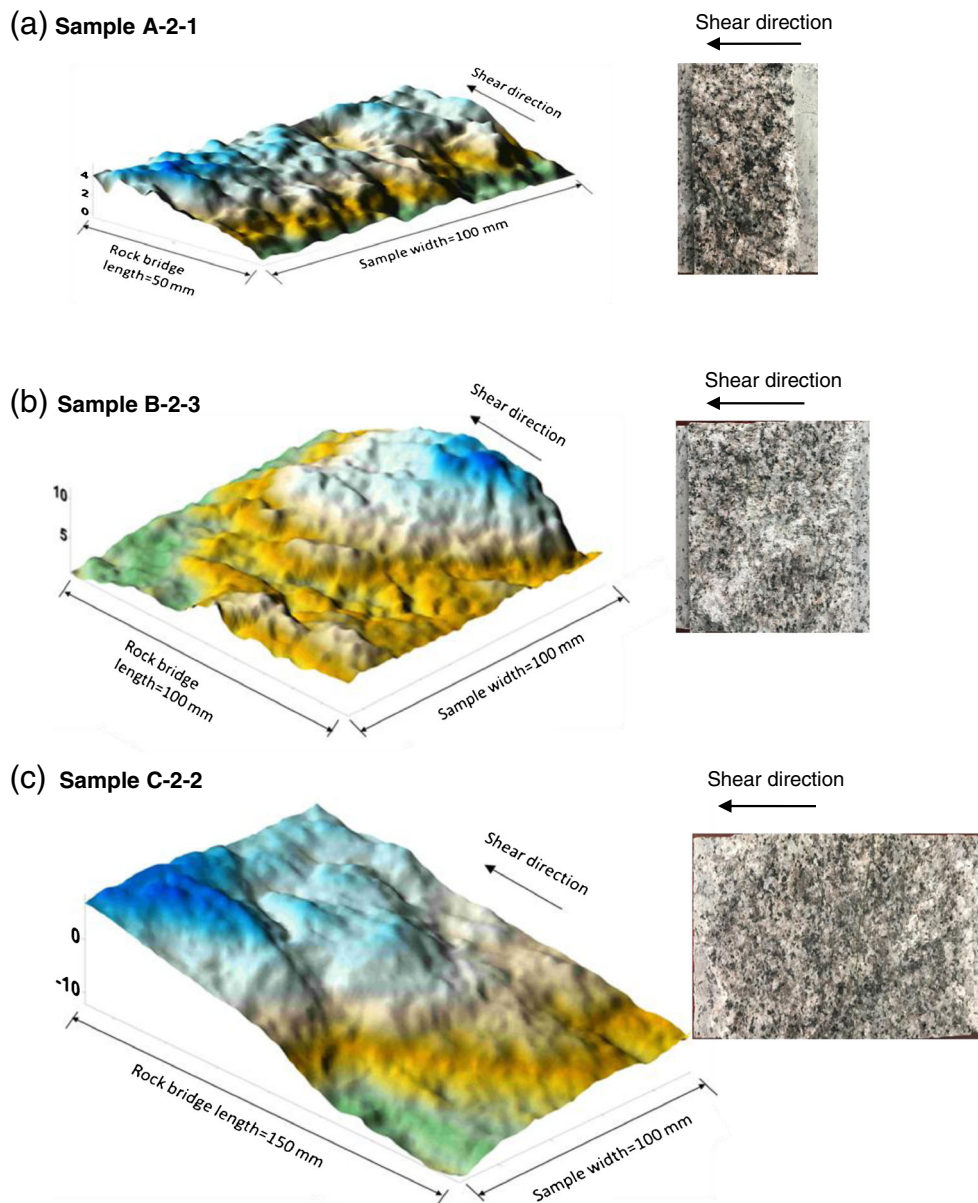
the joint persistency has increased from 0.25 to 0.75. This means that the shear strength reduction from the peak to residual increases as joint persistency decreases (see Fig. 5a, b).

After the direct shear test, the failure surfaces of the rock bridges got exposed, and their profile information was collected by using a Revscan 3D surface structure laser scanner available at the Shandong University of Science and Technology. The resolution of the spatial location of each point is $\pm 50 \mu\text{m}$, which guarantees obtaining the details of joint surface precisely. The whole failure surface of the rock bridge was carefully scanned. It has been shown in the literature that a sampling interval of less than 1 mm has the capability of scanning the mesoscopic features of a joint surface. Hence, a sampling interval of 0.5 mm was used to measure the joint roughness in three dimensions. Figure 10 displays the reconstructed failure surfaces of rock bridges resulting from the direct shear tests under the normal stress of 2.0 MPa. These failure surfaces clearly

Table 3 Peak shear strength and residual shear strength values of the granitic samples under different test scenarios

Joint persistency	Normal stress (MPa)	Sample number	Peak shear strength, τ_p (MPa)	Residual shear strength, τ_r (MPa)
$k = 0.75$	$\sigma_n = 2$ MPa	A-2-1	7.09	1.80
	$\sigma_n = 4$ MPa	A-4-1	10.74	2.87
	$\sigma_n = 6$ MPa	A-6-1	14.79	4.62
	$\sigma_n = 8$ MPa	A-8-2	16.13	5.51
$k = 0.50$	$\sigma_n = 2$ MPa	B-2-3	9.14	1.38
	$\sigma_n = 4$ MPa	B-4-2	14.16	3.45
	$\sigma_n = 6$ MPa	B-6-1	18.56	5.14
	$\sigma_n = 8$ MPa	B-8-3	22.13	5.68
$k = 0.25$	$\sigma_n = 2$ MPa	C-2-2	13.52	1.91
	$\sigma_n = 4$ MPa	C-4-1	15.53	2.84
	$\sigma_n = 6$ MPa	C-6-3	22.13	5.34
	$\sigma_n = 8$ MPa	C-8-1	27.46	6.67

Fig. 10 Failure surfaces of rock bridges for different joint persistency: **a** $k = 0.75$; **b** $k = 0.50$; **c** $k = 0.25$



show anisotropic roughness characteristics. Different fractal methodologies can be used to quantify such anisotropic surface roughness accurately (Kulatilake et al. 1998, 2006; Kulatilake and Um 1999; Ge et al. 2014). However, in this study, by incorporating the z_2 value proposed by Tse and Cruden (1979), the JRC values were estimated along the shear direction for different failure surfaces to quantify roughness in a simplified way. Tse and Cruden (1979) investigated the relation between z_2 and JRC based on the 10 Barton profiles and established an empirical equation to calculate the JRC using z_2 with a sampling interval of 0.5 mm. This equation is given as follows:

$$JRC = 32.2 + 32.47 \log z_2 \tag{2}$$

z_2 is expressed as

$$z_2 = \sqrt{\frac{1}{L_r} \int_{x=0}^{x=L_r} \left(\frac{dy}{dx}\right)^2 dx} = \sqrt{\frac{1}{N(\Delta x)^2} \sum_{i=1}^{N-1} (y_{i+2} - y_i)^2} \tag{3}$$

where L_r is the length of rock bridge; dx is the horizontal distance between two adjacent points along the sampling line; dy is the distance between adjacent points normal to the sampling line; x_i and y_i are the coordinates of an equally spaced sampling point i ; and N is the number of discrete measurement segments. Nine profiles parallel to the shear direction were extracted at every 10 mm of the joint surface width. The JRC value for the failure surface of the rock bridge was estimated as the average value of roughness of the nine profiles.

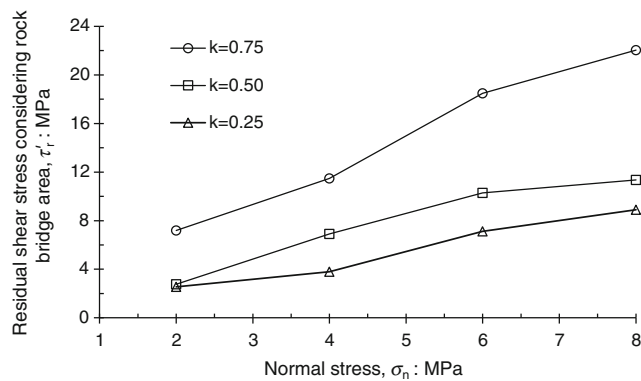


Fig. 11 Influence of joint persistency on the residual shear strength by considering only the rock bridge area of the rock joint

Accordingly, the JRC values for the failure surfaces of the rock bridges for the samples having $k = 0.75$, 0.50 , and 0.25 turned out to be 15.55 , 9.91 , and 8.45 , respectively. The failure surface seems to get rougher as the joint persistency increases. When the joint persistency is large (e.g., $k = 0.75$), the shear failure mode induces the crushed and pulverized coarse-grained material, which seems to make the failure surface rougher. On the other hand, when the joint persistency is small (e.g., $k = 0.25$), the tensile failure mode seems to produce a less rough surface compared to the case of high joint persistency due to the absence of the crushed and pulverized coarse-grained material. These findings are in good agreement with those obtained by Cheng et al. (2015) and Haeri et al. (2016). In addition, the failure surface roughness further influences the residual shear strength behavior. Figure 11 displays the residual shear strength by considering only the rock bridge area rather than the whole joint plane area. As shown in this figure, for a smaller rock bridge area (e.g., at $k = 0.75$), a higher roughness would induce a higher residual shearing capacity on a failure surface. For a larger rock bridge area (e.g., at $k = 0.25$), the low roughness accounts for its lower residual shear capacity on a failure surface.

Conclusions

In this study, a conceptual rock structure model was proposed to investigate the shear behavior of granite samples containing discontinuous joints through direct shear tests. Both joint persistency and normal stress level have a significant influence on the shear stress-shear displacement curves. The tested granitic discontinuous joint samples displayed typical brittle failure behavior. Possible influence of granitic material heterogeneity on the shear behavior was carefully evaluated by comparing the shear stress-shear displacement curves of the different samples subjected to the same testing scenarios. However, this influence was found to be negligible for the tested samples.

Test results indicated three failure modes in rock bridges that existed between the discontinuous joints: (a) shear failure mode, (b) compressive-shear failure mode, and (c) tensile failure. The failure mode depends on the joint persistency and normal stress level. Particularly, the shear failure mode was associated with relatively large joint persistency and low to moderate normal stress levels. The compressive-shear failure mode occurred for samples with large to moderate joint persistency and high normal stress level. The tensile failure mode occurred for samples with low joint persistency (i.e., large rock bridge length) irrespective of the normal stress level. These are new findings that do not appear in the rock mechanics literature.

The peak and residual shear strengths increase with the increment of normal stress level. Moreover, the peak shear strength and residual shear strength (based only on the rock bridge area) increase with the decrease of joint persistency. The roughness of the surfaces resulted from rock bridge rupturing was estimated through the 3D surface geometry laser scanning data and the JRC index. The JRC value was found to decrease with decreasing joint persistency. This is also a new finding that does not appear in the rock mechanics literature. The rock bridge failure surfaces with different JRC values would have significant influence on the residual shear behavior of the discontinuous joints in granitic materials.

Funding information The research reported in this manuscript was financially supported by the Natural Science Foundation of Shandong Province (Grant No. ZR2017BEE020). This research was also partially supported by the National Natural Science Foundation of China (Grant No. 51704183) and the Postdoctoral Science Foundation of China (Grant No. 2018M640646).

References

- Asadzadeh M, Moosavi M, Hossaini MF, Masoumi H (2018) Shear strength and cracking process of non-persistent jointed rocks: an extensive experimental investigation. *Rock Mech Rock Eng* 51: 415–428
- Bahaaddini M, Sharrock G, Hebblewhite BK (2013) Numerical direct shear tests to model the shear behavior of rock joints. *Comput Geotech* 51:101–115
- Bahaaddini M, Hagan PC, Mitra R, Khosravi MH (2017) Experimental and numerical study of asperity degradation in the direct shear test. *Eng Geol* 204:41–52
- Ban L, Qi CZ, Lu CS (2018) A direction-dependent shear strength criterion for rock joints with two new roughness parameters. *Arab J Geosci* 11:466
- Barton N (1973) Review of a new shear-strength criterion for rock joints. *Eng Geol* 7:287–332
- Cheng Y, Wong LNY, Zou CJ (2015) Experimental study on the formation of faults from en-echelon fractures in Carrara marble. *Eng Geol* 195:312–326
- Cui YF (2012) Direct shear failure of a synthetic rock containing discontinuous joints. Master thesis, University of Alberta, Edmonton, Alberta

- Ge YF, Kulatilake PHSW, Tang HM, Xiong CG (2014) Investigation of natural rock joint roughness. *Comput Geotech* 55:290–305
- Gehle C, Kutter HK (2003) Breakage and shear behavior of intermittent rock joints. *Int J Rock Mech Min Sci* 40:687–700
- Gerolymatou E, Triantafyllidis T (2016) Shearing of materials with intermittent joints. *Rock Mech Rock Eng* 49:2689–2700
- Ghazvinian A, Sarfarazi V, Schubert W, Blumel M (2012) A study of the failure mechanism of planar non-persistent open joints using PFC2D. *Rock Mech Rock Eng* 45:677–693
- Haeri H, Sarfarazi V, Lazemi HA (2016) Experimental study of shear behavior of planar non-persistent joint. *Comput Concret* 17:639–653
- ISRM (1978) Suggested methods for the quantitative description of discontinuities in rock masses. *Int J Rock Mech Min Sci* 15:319–368
- Kulatilake PHSW, Um J (1999) Requirements for accurate quantification of self-affine roughness using the roughness-length method. *Int J Rock Mech Min Sci* 36:1–18
- Kulatilake PHSW, Um J, Pan G (1998) Requirements for accurate quantification of self-affine roughness using the variogram method. *Int J Solids Struct* 35:4167–4189
- Kulatilake PHSW, Balasingam P, Park J, Morgan R (2006) Natural rock joint roughness quantification through fractal techniques. *Geotech Geol Eng* 24:1182–1202
- Lajtai EZ (1969) Strength of discontinuous rocks in direct shear. *Géotechn* 19:218–233
- Lajtai EZ, Carter BJ, Duncan EJS (1994) En echelon crack-arrays in potash salt rock. *Rock Mech Rock Eng* 27:89–111
- Li S, Feng XT, Li Z, Chen B, Zhang C, Zhou H (2012) In situ monitoring of rockburst nucleation and evolution in the deeply buried tunnels of Jinping II hydropower station. *Eng Geol* 137–138:85–96
- Paronuzzi P, Bolla A, Rigo E (2016) 3D stress-strain analysis of a failed limestone wedge influenced by an intact rock bridge. *Rock Mech Rock Eng* 49:3223–3242
- Sarfarazi V, Ghazvinian A, Schubert W, Blumel M, Nejati HR (2014) Numerical simulation of the process of fracture of echelon rock joints. *Rock Mech Rock Eng* 47:1355–1371
- Shang J, Hencher SR, West LJ (2016) Tensile strength of geological discontinuities including incipient bedding, rock joints and mineral veins. *Rock Mech Rock Eng* 49(11):4213–4225
- Sharma P, Verma AK, Negi A, Jha MK, Gautam P (2018) Stability assessment of jointed rock slope with different crack infillings under various thermomechanical loading. *Arab J Geosci* 11:431
- Tse R, Cruden DM (1979) Estimating joint roughness coefficients. *Int J Rock Mech Min Sci Geomech Abstr* 16:303–307
- Wong RHC, Lin P, Yu ZX, Tang CA, Chau KT (2002) Creeping damage around an opening in rock-like material containing non-persistent joints. *Eng Fract Mech* 69:2015–2027
- Wu Q, Xu YJ, Tang HM, Fang K, Jiang YF, Liu CY, Wang LQ, Wang XH, Kang JT (2018) Investigation on the shear properties of discontinuities at the interface between different rock types in the Badong formation, China. *Eng Geol* 245:280–291
- Yang XX, Qiao WG (2018) Numerical investigation of the shear behavior of granite materials containing discontinuous joints by utilizing the flat-joint model. *Comput Geotech* 104:69–80
- Yang XX, Kulatilake PHSW, Chen X, Jing HW, Yang SQ (2016) Particle flow modeling of rock blocks with nonpersistent open joints under uniaxial compression. *Int J Geomech* 16:04016020
- Yang XX, Jing HW, Tang CA, Yang SQ (2017) Effect of parallel joint interaction on mechanical behavior of jointed rock mass models. *Int J Rock Mech Min Sci* 92:40–53
- Yang XX, Jing HW, Qiao WG (2018) Numerical investigation of the failure mechanism of transversely isotropic rocks with a particle flow modeling method. *Processes* 6:171
- Zhao WH, Huang RQ, Yan M (2015) Study on the deformation and failure modes of rock mass containing concentrated parallel joints with different spacing and number based on smooth joint model in PFC. *Arab J Geosci* 8:7887–7897